

Multi-UAV Uniform Sweep Coverage in Unknown Environments: A Mergeable Nervous System (MNS)-Based Random Exploration

Aryo Jamshidpey¹ and Hugh H.-T. Liu¹

Abstract—This paper investigates the problem of multi-UAV uniform sweep coverage, where a homogeneous swarm of UAVs must collectively and evenly visit every portion of an unknown environment for a sampling task without having access to their own location and orientation. Random walk-based exploration strategies are practical for such a coverage scenario as they do not rely on localization and are easily implementable in robot swarms. We demonstrate that the Mergeable Nervous System (MNS) framework, which enables a robot swarm to self-organize into a hierarchical ad-hoc communication network using local communication, is a promising control approach for random exploration in unknown environments by UAV swarms. To this end, we propose an MNS-based random walk approach where UAVs self-organize into a line formation using the MNS framework and then follow a random walk strategy to cover the environment while maintaining the formation. Through simulations, we test the efficiency of our approach against several decentralized random walk-based strategies as benchmarks. Our results show that the MNS-based random walk outperforms the benchmarks in terms of the time required to achieve full coverage and the coverage uniformity at that time, assessed across both the entire environment and within local regions.

I. INTRODUCTION

Multi-UAV sweep coverage, where a group of UAVs collectively explore and cover an environment, has gained significant attention due to its direct impact on several practical applications. Tasks such as search and rescue [1], wildfire monitoring [2]–[4], and environmental surveillance [5] benefit significantly from efficient multi-UAV coverage strategies. This paper investigates a multi-UAV uniform sweep coverage task where a UAV swarm must collectively and evenly visit every portion of an unknown GNSS-denied environment—i.e., an environment where UAVs have no prior knowledge of its characteristics, including its shape and size, and do not have access to global positioning data to determine their location or orientation—to perform uniform sampling.

Typically, Random Walk exploration is practical for coverage in unknown GNSS-denied environments because it is a simple, scalable, flexible, and robust behavior that does not rely on localization or communication. Its ease of implementation makes it a suitable choice for robot swarms, enabling them to effectively explore unknown environments, although it may lead to increased repeated coverage [6]–[8]. To address this drawback, incorporating cooperative methods could help minimize redundancy and improve overall efficiency.

Building on our previous work [9], where we proposed the Mergeable Nervous Systems (MNS) [10], [11] as a suitable control approach for multi-robot sweep coverage with UGVs guided by UAVs, this paper, for the first time, applies this framework to a multi-UAV uniform sweep coverage task in an unknown GNSS-denied environment, focusing on random exploration using a homogeneous UAV swarm.

The MNS is a formation control framework that enables a robot team to achieve a degree of central coordination without sacrificing the benefits of decentralized control through a self-organizing process. More specifically, under this framework an aerial-ground swarm can self-organize into an ad hoc communication network with a hierarchical structure using vision-based relative positioning and local communication. The UAV that occupies the highest level of the hierarchy through self-organization is called the "brain" and is responsible for swarm-level decision-making and sending motion instructions downstream, while other robots use the network to cede authority to the brain and report sensing events upstream. By sending control information downstream, the robots establish a target formation and maintain it as the brain moves, facilitating effective exploration.

In this paper, we demonstrate that the MNS framework is an effective control approach for achieving multi-UAV uniform sweep coverage in unknown GNSS-denied environments. Before that, as a proof of concept for the effectiveness of the MNS in multi-UAV coverage, we illustrate how a UAV swarm utilizes this framework to achieve uniform coverage in a simple convex environment by forming a line formation, a common shape suitable for sweeping and mapping tasks [12], and executing standard back-and-forth boustrophedon motions [13], [14].

Building on this, we introduce an MNS-based random walk approach where UAVs, maintaining a line formation, employ a random walk strategy to cover the environment. The main objective of our research is to demonstrate that, even with random exploration in unknown settings, an MNS-based method can outperform common decentralized random walk-based approaches in multi-UAV coverage.

We validate this by comparing the performance of our MNS-based random walk approach against four decentralized cooperative and non-cooperative random walk-based approaches as benchmarks in simulated experiments. Our results indicate that the MNS-based random walk achieves superior performance, reducing the time to achieve full coverage and improving coverage uniformity across the entire environment and within local regions.

¹Aryo Jamshidpey and Hugh H.-T. Liu are with the University of Toronto Institute for Aerospace Studies (UTIAS), Toronto, Canada, aryo.jamshidpey@utoronto.ca hugh.liu@utoronto.ca

II. RELATED WORK

Coverage has been extensively studied in wireless sensor networks and robotics and is typically classified into continuous coverage and sweep coverage [15], [16]. Continuous coverage can be further divided into point coverage, area coverage, and barrier coverage and involves stationary robots continuously monitoring the entire environment, which can be impractical for large environments due to the high number of robots required. In contrast, sweep coverage uses mobile robots that move throughout the environment to visit every portion, making it more practical with a smaller robot team. This study focuses on sweep coverage, also referred to as coverage path planning (CPP) [8], [17], [18]. CPP methods can be categorized into offline and online approaches based on their knowledge of the environment [17]. Offline methods require prior knowledge to pre-plan paths [19], [20], while online methods are sensor-based and adapt to uncertain environments without any prior information [21], [22].

Random walk as an online sweep coverage technique is widely recognized in swarm robotics, particularly in scenarios where robots lack access to their location and orientation and have no prior knowledge of the environment [8]. Random walk refers to a movement pattern in which agents independently move in random directions and randomly change direction either at intervals or upon encountering boundaries or obstacles. Various random walk strategies have been explored for environmental exploration and coverage tasks [6], [7]. In [6], the authors compared five random walk strategies for swarm mapping in unknown environments, including Brownian motion [23], correlated random walk [24], Lévy walk [25], Lévy taxis [26], and ballistic motion (equivalent to Random Billiards [27]). These methods are categorized in the literature as either fully random or specialized in coverage or exploration tasks. The study found that random billiards significantly outperforms other methods due to its higher coverage speed.

Using virtual pheromones is a common approach to reduce redundant coverage, based on which agents avoid revisiting recently explored areas [28]–[30]. This approach relies on implicit communication through virtual pheromones, where agents do not communicate directly but instead leave pheromone cues in the environment for other agents to detect. In [31], an efficient pheromone-based method for sweep coverage by UAVs was proposed, which has been adapted to our scenario. In another study [32], a UAV swarm was employed for weed coverage and mapping in farmlands, utilizing a reinforced random walk [33], and both explicit communication and pheromone-based cooperation. However, this approach is unsuitable for our GNSS-denied scenario because it relies on UAVs having knowledge of a predefined grid and requires communicating positional information about visited cells. Finally, a connectivity-aware pheromone-based model for UAV networks was proposed, requiring UAVs to communicate their positions to maintain network connectivity [34]. While this method is useful for maintaining connectivity, it is not feasible for coverage tasks

in GNSS-denied environments, as it relies on position sharing among UAVs.

III. PROBLEM STATEMENT

This research addresses the problem of multi-UAV sweep coverage, where a homogeneous swarm of camera-equipped UAVs must collectively and evenly visit every portion of an unknown GNSS-denied environment to perform a uniform sampling task. The task, defined as taking one picture per each portion of the environment (with each portion representing a non-overlapping area of one square meter), requires UAVs to fly at a specific constant altitude (sampling altitude) and with a linear velocity not exceeding a target value, referred to as the target sampling velocity. While UAVs can fly at various velocities and altitudes, sampling is only valid when they adhere to these specific conditions.

In this research, for simplicity, we represent the environment as a square arena, a common practice in the literature, conceptually decomposed into $1\text{ m} \times 1\text{ m}$ cells (i.e., the portions defined by the sampling task). This decomposition facilitates the performance evaluation of the studied methods; however, the UAVs are unaware of this grid and must operate without relying on it. A cell is considered visited only when a UAV enters it while performing the sampling task and adhering to the required speed and altitude conditions. Otherwise, the cell is not considered visited.

IV. METHODS

In this section, we detail the two MNS-based and four benchmark decentralized approaches used in our study, followed by the simulation setup. To ensure a fair comparison, all random walk-based approaches are built upon a core behavior rooted in a consistent random walk strategy. We use Random Billiards as the core behavior for all random walk-based strategies due to its demonstrated efficiency in exploration tasks [27], [35]. More specifically, Random Billiards is one of the fastest random walk strategies and involves each agent moving straight at a constant velocity until reflecting off a boundary in a random direction.

Additionally, two of our benchmark cooperative approaches are adapted from the concept of swarm dispersion [36]–[39], a strategy commonly employed in continuous area coverage to maximize inter-agent distance and enhance the overall monitored area. Here, we adapted this concept to reduce UAV densities in local regions.

Finally, for all the approaches, parameters were fine-tuned during an initial testing phase to ensure they performed well for comparison.

A. MNS-BASED BOUSTROPHEDON SWEEP

The MNS-based Boustrophedon Sweep approach (MNS-BS) extends our previous work on the MNS framework for sweep coverage [9], [35], initially designed for a heterogeneous swarm that self-organizes into a hierarchical ad-hoc communication network with a caterpillar tree topology and a linear formation. In the previous setup, the brain UAV served as the root of the tree, the ground robots acted as

the leaf nodes, and the intermediate UAV nodes functioned as supervisors for a subset of ground robots while also being guided by another UAV.

In this extension, we adapt the framework to a homogeneous UAV swarm. Before starting the coverage task, UAVs are positioned at two different flight altitudes, referred to as supervisory and sampling altitudes. UAVs establish a hierarchical ad-hoc communication network with a caterpillar tree topology using the same self-organizing process as in the previous version, forming a line formation (as depicted in Fig. 1). In this hierarchical structure, the sampling UAVs act as the leaves and perform the coverage task under the supervision of the UAVs flying at the supervisory altitude. The distance between each pair of neighboring sampling UAVs is determined based on the side length of the portions defined by the sampling task; in our scenario, it is set to 1 m, corresponding to the side length of each portion (which is a 1 m x 1 m cell). This configuration aims to minimize gaps and overlap in coverage, ensuring no cell is missed between two sampling UAVs. Here, we use 25 UAVs for our sweep coverage task: 5 serve as supervisors (including the brain), and 20 function as sampling UAVs. However, as demonstrated in our previous work, the MNS is scalable and supports various setups.

To establish and maintain a target formation during motion, each child in the network cedes authority to its parent UAV, which can track the child's motion and guide it to a relative position and orientation, as detailed in [43]. At each step, each UAV receives motion instructions from its parent, specifying the child's current orientation represented by quaternion (q_t) and the desired relative linear velocity (v) and angular velocity (ω). The parent UAV senses its child's current displacement (d_t) and orientation (q_t) and determines these motion instructions for the child as follows:

$$\mathbf{v} = k_1 \left(\frac{\mathbf{d}_{t+1} - \mathbf{d}_t}{\|\mathbf{d}_{t+1} - \mathbf{d}_t\|} \right), \quad \omega = k_2 \cdot f(\mathbf{q}_{t+1} \times \mathbf{q}_t^{-1}), \quad (1)$$

where $f(x)$ is a function that converts a quaternion to an Euler angle, and k_1 and k_2 are speed coefficients.

After establishing the formation, the brain UAV executes standard back-and-forth boustrophedon motions (Fig. 1), following the target sampling velocity. A line formation is a common shape suitable for sweeping and mapping tasks [12], and back-and-forth motions are effective for coverage in convex environments [13], [14]. This ensures that every cell in the environment is visited by the sampling UAVs.

Whenever the brain reaches a boundary, the MNS exits the boundary by 50 cm, shifts by the length of the formation, and begins a new sweep. This process ensures that each cell is visited exactly once, making the approach deterministic with a guaranteed completion time.

B. MNS-BASED RANDOM WALK

In the MNS-based Random Walk approach (MNS-RW), UAVs first self-organize into the same hierarchical network with line formation used in MNS-BS. Then, the brain UAV moves straight forward in a random direction at the target

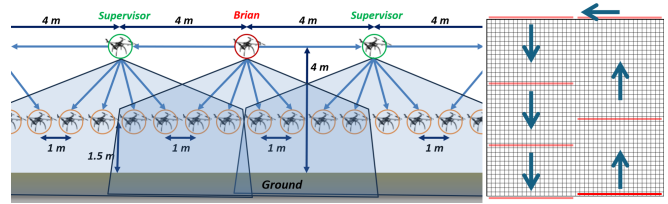


Fig. 1. UAV positions in the formation and network topology for the MNS-based approaches (left), and MNS-BS sweep strategy (right).

sampling velocity, followed by the other UAVs, until it reaches a boundary. As mentioned earlier, in the MNS framework, the formation is consistently maintained throughout the brain's movement, including during the brain's rotations.

Upon reaching a boundary, the brain continues moving straight forward, crossing the boundary until it is more than 95 cm away. At this point, it selects a random relative orientation, θ_{rand} , directed towards the interior of the arena, excluding any orientation within a 30° offset from its reciprocal heading. The brain then chooses the rotation direction, D_{rand} (clockwise or counterclockwise), which requires the least time to reach the selected orientation.

If the rotation direction D_{rand} is the same as the optimal rotation direction for aligning the formation along the boundary, denoted as D_{adjust} , the brain adjusts the formation accordingly. This adjustment is performed by rotating at an angular velocity that ensures no sampling UAV exceeds the target sampling velocity while maintaining the formation. During this phase, the UAVs continue to perform the sampling task as their velocities remain within the allowed range.

After either adjusting the formation along the boundary (when D_{rand} is the same as D_{adjust}) or determining no adjustment is necessary (if D_{rand} is not the same as D_{adjust}), the brain UAV rotates to the randomly selected orientation, θ_{rand} . During this "Preparation" phase, the sampling task is temporarily paused, allowing UAVs to exceed the target sampling velocity to reposition effectively.

After reaching the randomly selected orientation, θ_{rand} , the brain resumes moving straight forward, continuing the random walk.

C. RANDOM BILLIARDS WITH RANDOMIZED OBSTACLE AVOIDANCE

In the Random Billiards with Randomized Obstacle Avoidance strategy (RB), each UAV moves straight forward with the target sampling velocity unless it encounters a boundary or obstacle. When a UAV is within 5 cm of a boundary, it selects a random relative orientation directed towards the interior of the arena, avoiding directions within a 5° offset from its reciprocal heading.

The strategy includes two obstacle avoidance behaviors: a short-range avoidance with higher priority and a medium-range avoidance with lower priority. For short-range avoidance, if a UAV detects an obstacle within a 1 m radius and within 90° of its heading, it selects a random orientation offset between 10° and 30° . For medium-range avoidance,

if a UAV detects an obstacle within a 2.5 m radius and within 60° of its heading, it selects a random orientation offset between 5° and 70°.

In both cases, the UAV turns clockwise if the obstacle is on the left and counterclockwise if it is on the right. After completing the rotation, if no obstacles or boundaries are detected, the UAV resumes moving straight forward following the target sampling velocity.

D. LOCAL DENSITY REDUCTION THROUGH COMMUNICATION AND RANDOM REACTIONS

In the Local Density Reduction through Communication and Random Reactions approach (LDR-Random), UAVs utilize RB as their core behavior. In addition to this core behavior, UAVs attempt to reduce local density by using wireless communication with their neighbors to achieve a more uniform distribution throughout the arena. Each UAV broadcasts its ID within a 10m communication range at each step. If a UAV receives at least five distinct IDs in a step, it determines that the local density is high and sends a message to its neighbors within the same communication range, notifying them of this condition.

Upon receiving a high-density notification, the UAV randomly rotates between 70° and 90° in a clockwise direction. Following this reaction, the UAV deactivates its density reduction behavior for 50 steps and resumes its core behavior (i.e., RB). Additionally, after completing any obstacle avoidance reaction or reacting to a boundary, a UAV deactivates its density reduction behavior for 350 steps.

E. LOCAL DENSITY REDUCTION THROUGH COMMUNICATION AND REPULSIVE REACTIONS

In the Local Density Reduction through Communication and Repulsive Reactions approach (LDR-Repulsive), UAVs utilize RB as their core behavior, similar to LDR-Random. Additionally, this approach requires each UAV to accurately estimate the position of the sender of any received message within its local reference frame. This capability enables a more precise density reduction strategy.

In this approach, each UAV broadcasts its ID within a 5 m communication range at each step. If a UAV receives at least three distinct IDs within a step, it sends a message to its neighbors within the same communication range, informing them of this condition.

Once a UAV receives such a message, it independently calculates the average position of its neighbors (i.e., the UAVs from which it received messages in the current step). The UAV then determines the vector from its current position to that average position and calculates the opposite direction. Next, it selects the rotation direction that minimizes the time needed to reach that opposite direction and rotates accordingly until it reaches that direction. After completing such a rotation or an obstacle avoidance, the UAV deactivates its density reduction behavior for 350 steps and resumes its core behavior (i.e., RB).

F. PHEROMONE-BASED MOBILITY MODEL

The Pheromone-Based Mobility Model (PM), adapted from [31], utilizes RB as its core behavior, similar to LDR-Random and LDR-Repulsive. The use of PM, although artificial pheromones are difficult to implement in practice, serves as a benchmark for minimizing repeated coverage in sweep coverage task. Each UAV deposits 5000 units of virtual pheromone upon visiting a cell, which evaporates at a rate of 1 unit per step. UAVs can read the pheromone levels in their current cell and neighboring cells to guide their movement decisions.

When no pheromone is detected ahead, UAVs move straight forward at the target sampling velocity. If pheromone is detected and the pheromone response is active, UAVs choose their next direction based on the probabilities shown in Table I, which depend on the amounts of pheromone sensed to the 'left,' 'right,' and 'ahead.' 'total' is the sum of these values (total = left + ahead + right).

If a UAV decides to turn left or right, it executes a 45° turn in the selected direction before resuming forward motion. After completing a pheromone-based reaction, the UAV deactivates its pheromone response for 25 steps. Additionally, after performing an obstacle avoidance or reacting to a boundary, the UAV deactivates its pheromone response for 50 steps.

TABLE I
PHEROMONE ACTION PROBABILITIES FOR UAV MOVEMENT.

Go Ahead	Go Right	Go Left
$p_A = \frac{\text{total} - \text{ahead}}{2 \times \text{total}}$	$p_R = \frac{\text{total} - \text{right}}{2 \times \text{total}}$	$p_L = \frac{\text{total} - \text{left}}{2 \times \text{total}}$

G. SIMULATION SETUP

The simulations were conducted in the ARGoS simulator [40], using UAV models implemented with an existing plugin [41], [42]. The simulation took place in a 40 m x 40 m square arena, centered at (0,0) in the coordinate frame. For each approach, 30 simulation runs were conducted with 25 UAVs. The sampling altitude, supervisory altitude, and target sampling velocity were set to 1.5 m, 4 m, and 1 m/s, respectively, with a communication range of up to 10 m. For the MNS-based approaches, the initial steps allow the formation to self-organize. Once the formation is established, the brain UAV is positioned at (10 m, -19.5 m, 4 m) for MNS-BS (with the entire formation aligned along the southern boundary) and at (20 m, -20 m, 4 m) for MNS-RW (above the southeastern corner), with the entire formation turned to match the brain UAV's randomly selected orientation toward the interior. For decentralized approaches, UAVs are randomly and uniformly placed within a 3 m x 20 m area located inside the square arena along the middle of the southern boundary, at the 1.5 m flight altitude. UAVs start with a minimum spacing of 1.5 m and random orientations between 0° and 180°, all facing the interior. These initial

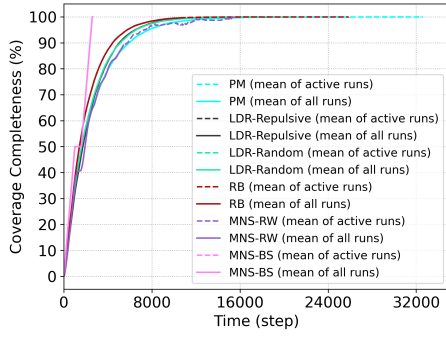


Fig. 2. Average coverage completeness of each approach over time.

steps are not recorded in the data. The dataset is available at <https://doi.org/10.5281/zenodo.13764325>.

V. SIMULATION RESULTS

In this section, we present the results of our simulations, evaluating three key metrics: coverage completion time (CCT), total coverage uniformity at coverage completion (TCU), and local coverage uniformity at that time (LCU).

A. COVERAGE COMPLETION TIME (CCT)

We evaluate the performance of the six approaches in terms of coverage completion time (CCT), defined as the number of steps required to achieve full coverage of the environment (see Fig. 3(a) and Table II), and the coverage progress rate over time, noted as CPR (see Fig. 2).

From Figs. 2 and 3(a) and the minimal CCT value in Table II, MNS-BS substantially outperforms all other approaches in both average CPR and CCT (2,614 steps with no variability).

The mean CPR for MNS-RW is nearly the same as PM but slightly worse than RB and LDR approaches (see Fig. 2). The longer runs of MNS-RW likely affect its average CPR negatively, but its mean CCT (10,194.467 steps) is significantly lower than all decentralized approaches, as evidenced by Fig. 3(a) and Table II. As seen in Fig. 3(a), most runs of MNS-RW have a lower CCT than the decentralized approaches.

For the benchmark decentralized approaches, as time progresses, UAVs encounter more difficulty locating the remaining unvisited cells (see Fig. 2). Among these approaches, RB demonstrates the highest mean CPR and the lowest mean CCT (15,420.000 steps) as seen in Figs. 2 and 3(a) and Table II. The average CPR of LDR-Random and LDR-Repulsive are similar and slightly better than PM. In terms of mean CCT, PM performs the worst (22,332.800 steps), while LDR approaches are comparable. LDR-Repulsive slightly outperforms LDR-Random in terms of mean CCT (16,059.233 steps vs. 16,580.067 steps).

B. TOTAL COVERAGE UNIFORMITY AT THE COVERAGE COMPLETION TIME (TCU)

Coverage uniformity is defined as a measure of the variability in the number of visits across all cells in the

TABLE II
MEAN AND STANDARD DEVIATION OF PERFORMANCE METRICS.

Approach	CCT	SD-CCT	TCU	SD-TCU	LCU	SD-LCU
MNS-BS	2614.000	0	0	0	0	0
MNS-RW	10194.467	2376.935	-1.244	0.247	-0.862	0.219
PM	22332.800	3961.065	-1.566	0.166	-1.397	0.204
LDR-RP	16059.233	1555.650	-2.0241	0.121	-1.882	0.236
LDR-R	16580.067	2220.828	-2.030	0.168	-1.899	0.269
RB	15420.000	3581.138	-2.093	0.284	-1.950	0.327

environment. An optimal coverage strategy would have no variability, meaning all cells are visited an equal number of times. For each simulation run, let $v_i \in \mathbf{v}$ represent the total number of visits to cell i . The coverage uniformity ρ is calculated as the negative mean absolute deviation of \mathbf{v} from its median, given by:

$$\rho = -\frac{\sum_{i=1}^c |v_i - M(\mathbf{v})|}{c}, \quad (2)$$

where c is the number of cells and $M(\mathbf{v})$ is the median of \mathbf{v} . A higher value of ρ indicates greater uniformity, with the ideal case being $\rho = 0$, where every cell is visited equally.

As shown in Fig.3(b) and the corresponding values in TableII, MNS-BS achieves the best possible total coverage uniformity (TCU), with $\rho = 0$ and no variability.

Among the random walk-based approaches, MNS-RW demonstrates the highest mean TCU (-1.244), outperforming all decentralized approaches. The PM approach follows with a mean TCU of -1.566, making it the most uniform decentralized approach. The three other decentralized strategies, LDR-Repulsive, LDR-Random, and RB, trail behind with mean TCU values of -2.024, -2.030, and -2.093, respectively, indicating less uniform coverage distribution. Among these, LDR-Repulsive shows a marginally better performance compared to the others, while RB exhibits the lowest TCU.

C. LOCAL COVERAGE UNIFORMITY AT THE COVERAGE COMPLETION TIME (LCU)

We assess the coverage uniformity within each 10 m x 10 m region of the environment at coverage completion using the same uniformity equation 2. This metric provides insight into how evenly coverage is achieved across smaller areas within the environment.

As shown in Fig. 3(c) and Table II, MNS-BS considerably outperforms all other approaches in local uniformity, achieving a value of 0 with no variability, which indicates perfect uniformity in each local area.

Among the random Walk-based approaches, MNS-RW achieves the highest LCU (-0.862), significantly outperforming the fully decentralized approaches. The PM approach follows with a mean LCU of -1.397, making it the best-performing decentralized approach in this metric. Among the three remaining decentralized strategies, LDR-Repulsive, LDR-Random, and RB exhibit LCU values of -1.882, -1.899, and -1.950, respectively, with LDR-Repulsive and LDR-Random performing slightly better than RB.

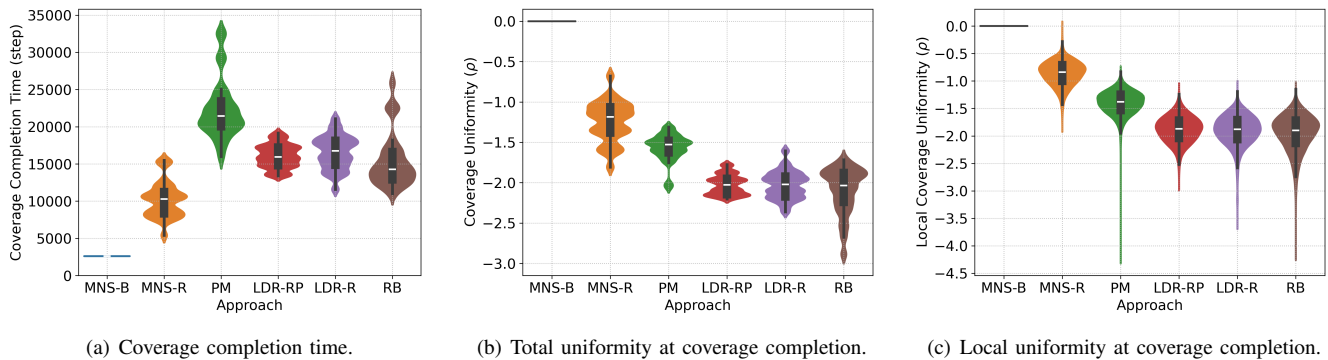


Fig. 3. Coverage performance results. LDR-R and LDR-RP represent LDR-Random and LDR-Repulsive, respectively.

A notable observation is the higher ratio of mean TCU to mean LCU for MNS-RW (approximately 1.44) compared to the decentralized approaches, where the ratio is around 1.12 for PM and approximately 1.07 for the other three decentralized approaches. This higher ratio suggests a more significant improvement in local uniformity relative to total uniformity for MNS-RW, highlighting the positive impact of the MNS framework on enhancing local uniformity.

VI. DISCUSSIONS AND CONCLUSIONS

In this study, we evaluated the performance of six approaches for multi-UAV sweep coverage in unknown, GNSS-denied environments. MNS-BS extremely outperforms the other approaches in terms of CCT, TCU, and LCU. The deterministic nature of MNS-BS, coupled with its effective line formation and back-and-forth motion strategy, ensures that every cell is visited exactly once, achieving perfect uniformity with no variability.

Focusing on the random walk-based methods, MNS-RW demonstrates superior performance across all metrics compared to the decentralized approaches. It achieves the best TCU and LCU, with a higher ratio of mean TCU to mean LCU compared to other approaches. This indicates that MNS-RW is particularly effective in distributing coverage more evenly across smaller areas, which could be advantageous in scenarios where local uniformity is crucial. Although MNS-RW does not outperform in terms of variability in all 3 metrics, its corresponding mean, maximum, and minimum values are significantly better than those of the decentralized approaches, indicating a much faster and more reliable approach overall.

PM is the most uniform decentralized approach, achieving good TCU and LCU. However, this comes at the cost of time; PM has the slowest CCT among all approaches. The effectiveness of PM in achieving uniform coverage is well-established in the literature, but its slower progress highlights the trade-off between uniformity and speed in decentralized coverage strategies.

Among the decentralized approaches, RB demonstrates the lowest mean CCT and the highest mean CPR. However, RB has the lowest consistency (highest variability) across all three metrics, which can lead to less reliable performance

in varied environments. LDR-Repulsive and LDR-Random show comparable results in terms of mean TCU and LCU, but LDR-Repulsive has the lowest variability, making it the most consistent decentralized approach. However, this consistency requires the assumption that UAVs can accurately estimate the relative position of their neighbors upon receiving a message, which may not be realistic.

While MNS-RW has a slightly lower mean CPR compared to the fastest decentralized approach, RB, several factors contribute to this outcome. In our MNS setup, only 20 out of 25 UAVs are active as sampling UAVs, and MNS-RW allows UAVs to cross the environment's borders to perform turns and select new directions. Consequently, for a significant amount of time, a large portion of the MNS may fly outside the arena, resulting in fewer active sampling UAVs within the environment and occasionally leading to a lower CPR compared to the benchmark approaches. Future work could explore adaptive MNS-based random walk strategies that dynamically adjust the formation upon detecting a boundary, combining advanced shifts and curved back-and-forth sweeps while ensuring all UAVs remain within the environment, thereby improving overall performance.

Reducing density using LDR approaches results in higher consistency in performance across all metrics without necessarily improving the mean values for CCT, TCU, and LCU, and often at the cost of time compared to RB. This finding is influenced by the resolution of the decomposition (cell size). If larger cells were considered or if cells were marked as visited when within the UAV's field of view rather than being physically entered, density reduction would likely improve CCT, TCU, and LCU. However, in our setup, UAVs might miss visiting an unvisited cell due to their reactions, which can lead to increased coverage time. An adaptive density reduction strategy could be another avenue for future exploration to further improve performance.

In summary, MNS-BS excels in our scenario as expected. MNS-RW shows better performance than decentralized approaches in all three metrics and is particularly advantageous where local uniformity is a priority. PM offers the best uniformity among the decentralized approaches, but at a significant time cost, and RB provides a fast but inconsistent with low uniformity. LDR approaches improve consistency.

REFERENCES

- [1] M. Senanayake, I. Senthooan, and et al., "Search and tracking algorithms for swarms of robots: A survey," *Robotics and Autonomous Systems*, vol. 75, no. Part B, pp. 422–434, 2016.
- [2] H. X. Pham, H. M. La, D. Feil-Seifer, and M. Deans, "A distributed control framework for a team of unmanned aerial vehicles for dynamic wildfire tracking," in *2017 IEEE/RSJ international conference on intelligent robots and systems (IROS)*, pp. 6648–6653, IEEE, 2017.
- [3] D. W. Casbeer, D. B. Kingston, R. W. Beard, and T. W. McLain, "Cooperative forest fire surveillance using a team of small unmanned air vehicles," *International journal of systems science*, vol. 37, no. 6, pp. 351–360, 2006.
- [4] Z. Lin and H. H. Liu, "Topology-based distributed optimization for multi-uav cooperative wildfire monitoring," *Optimal Control Applications and Methods*, vol. 39, no. 4, pp. 1530–1548, 2018.
- [5] N. Basilico and S. Carpin, "Deploying teams of heterogeneous uavs in cooperative two-level surveillance missions," in *2015 IEEE/RSJ International Conference on Intelligent Robots and Systems (IROS)*, pp. 610–615, IEEE, 2015.
- [6] M. Kegeleirs, D. Garzón Ramos, and M. Birattari, "Random walk exploration for swarm mapping," in *Annual conference towards autonomous robotic systems*, pp. 211–222, Springer, 2019.
- [7] C. Dimidov, G. Oriolo, and V. Trianni, "Random walks in swarm robotics: an experiment with kilobots," in *International conference on swarm intelligence*, pp. 185–196, Springer, 2016.
- [8] C. S. Tan, R. Mohd-Mokhtar, and M. R. Arshad, "A comprehensive review of coverage path planning in robotics using classical and heuristic algorithms," *IEEE Access*, vol. 9, pp. 119310–119342, 2021.
- [9] A. Jamshidpey, W. Zhu, M. Wahby, M. Allwright, M. K. Heinrich, and M. Dorigo, "Multi-robot coverage using self-organized networks for central coordination," in *International Conference on Swarm Intelligence*, pp. 216–228, Springer, 2020.
- [10] W. Zhu, M. Allwright, M. K. Heinrich, S. Oğuz, A. L. Christensen, and M. Dorigo, "Formation control of uavs and mobile robots using self-organized communication topologies," in *International conference on swarm intelligence*, pp. 306–314, Springer, 2020.
- [11] W. Zhu, S. Oğuz, M. K. Heinrich, M. Allwright, M. Wahby, A. L. Christensen, E. Garone, and M. Dorigo, "Self-organizing nervous systems for robot swarms," *arXiv preprint arXiv:2401.13103*, 2024.
- [12] Y. Liu and R. Bucknall, "A survey of formation control and motion planning of multiple unmanned vehicles," *Robotica*, vol. 36, no. 7, pp. 1019–1047, 2018.
- [13] A. Jamshidpey, M. Dorigo, and M. K. Heinrich, "Reducing uncertainty in collective perception using self-organizing hierarchy," *Intelligent Computing*, vol. 2, p. 0044, 2023.
- [14] H. Choset and P. Pignon, "Coverage path planning: The boustrophedon cellular decomposition," in *Field and service robotics*, pp. 203–209, Springer, 1998.
- [15] R. Elhabyan, W. Shi, and M. St-Hilaire, "Coverage protocols for wireless sensor networks: Review and future directions," *Journal of Communications and Networks*, vol. 21, no. 1, pp. 45–60, 2019.
- [16] B. Gorain and P. S. Mandal, "Approximation algorithms for sweep coverage in wireless sensor networks," *Journal of parallel and Distributed Computing*, vol. 74, no. 8, pp. 2699–2707, 2014.
- [17] E. Galceran and M. Carreras, "A survey on coverage path planning for robotics," *Robotics and Autonomous Systems*, vol. 61, no. 12, pp. 1258–1276, 2013.
- [18] T. M. Cabreira, L. B. Brisolará, and F. J. Paulo R., "Survey on coverage path planning with unmanned aerial vehicles," *Drones*, vol. 3, no. 1, p. 4, 2019.
- [19] B. Jia, Z. Gao, J. Jing, B. Huang, S. Liu, K. Muhammad, and J. J. P. C. Rodrigues, "Coverage path planning for iouavs with tiny machine learning in complex areas based on convex decomposition," *IEEE Internet of Things Journal*, vol. 11, no. 12, pp. 21103–21111, 2024.
- [20] M. Hassan and D. Liu, "Ppcpp: A predator-prey-based approach to adaptive coverage path planning," *IEEE Transactions on Robotics*, vol. 36, no. 1, pp. 284–301, 2020.
- [21] W. Hu, Y. Yu, S. Liu, C. She, L. Guo, B. Vucetic, and Y. Li, "Multi-uav coverage path planning: A distributed online cooperation method," *IEEE Transactions on Vehicular Technology*, vol. 72, no. 9, pp. 11727–11740, 2023.
- [22] J. Song and S. Gupta, " ε^* : An online coverage path planning algorithm," *IEEE Transactions on Robotics*, vol. 34, no. 2, pp. 526–533, 2018.
- [23] R. P. Feynman, R. B. Leighton, and M. Sands, "Mainly mechanics, radiation, and heat," (*No Title*), 1963.
- [24] E. Renshaw and R. Henderson, "The correlated random walk," *Journal of Applied Probability*, vol. 18, no. 2, pp. 403–414, 1981.
- [25] V. Zaburdaev, S. Denisov, and J. Klafter, "Lévy walks," *Reviews of Modern Physics*, vol. 87, no. 2, pp. 483–530, 2015.
- [26] Z. Pasternak, F. Bartumeus, and F. W. Grasso, "Lévy-taxis: a novel search strategy for finding odor plumes in turbulent flow-dominated environments," *Journal of Physics A: Mathematical and Theoretical*, vol. 42, no. 43, p. 434010, 2009.
- [27] F. Comets, S. Popov, G. M. Schütz, and M. Vachkovskaia, "Billiards in a general domain with random reflections," *Archive for rational mechanics and analysis*, vol. 191, no. 3, pp. 497–537, 2009.
- [28] M. Dorigo, "Optimization, learning and natural algorithms," *Ph. D. Thesis, Politecnico di Milano*, 1992.
- [29] M. Rosalie, G. Danoy, S. Chaumette, and P. Bouvry, "Chaos-enhanced mobility models for multilevel swarms of uavs," *Swarm and evolutionary computation*, vol. 41, pp. 36–48, 2018.
- [30] S. S. Ge and C.-H. Fua, "Complete multi-robot coverage of unknown environments with minimum repeated coverage," in *Proceedings of the 2005 IEEE International Conference on Robotics and Automation*, pp. 715–720, IEEE, 2005.
- [31] E. Kuiper and S. Nadjm-Tehrani, "Mobility models for uav group reconnaissance applications," in *2006 International Conference on Wireless and Mobile Communications (ICWMC'06)*, pp. 33–33, IEEE, 2006.
- [32] D. Albani, D. Nardi, and V. Trianni, "Field coverage and weed mapping by uav swarms," in *2017 IEEE/RSJ International Conference on Intelligent Robots and Systems (IROS)*, pp. 4319–4325, Ieee, 2017.
- [33] A. Stevens and H. G. Othmer, "Aggregation, blowup, and collapse: the abc's of taxis in reinforced random walks," *SIAM Journal on Applied Mathematics*, vol. 57, no. 4, pp. 1044–1081, 1997.
- [34] S. Devaraju, A. Ihler, and S. Kumar, "A connectivity-aware pheromone mobility model for autonomous uav networks," in *2023 IEEE 20th Consumer Communications & Networking Conference (CCNC)*, pp. 1–6, IEEE, 2023.
- [35] A. Jamshidpey, M. Wahby, M. K. Heinrich, M. Allwright, W. Zhu, and M. Dorigo, "Centralization vs. decentralization in multi-robot coverage: Ground robots under uav supervision," *arXiv preprint arXiv:2408.06553*, 2024.
- [36] J. Bayert and S. Khorbotly, "Robotic swarm dispersion using gradient descent algorithm," in *2019 IEEE International Symposium on Robotic and Sensors Environments (ROSE)*, pp. 1–6, IEEE, 2019.
- [37] M. Vijay, M. Kuber, and K. Sivayazi, "Received signal strength based dispersion of swarm of autonomous ground vehicles," in *2017 2nd IEEE International Conference on Recent Trends in Electronics, Information & Communication Technology (RTEICT)*, pp. 52–57, IEEE, 2017.
- [38] J. Beal, "Superdiffusive dispersion and mixing of swarms with reactive levy walks," in *2013 IEEE 7th International Conference on Self-Adaptive and Self-Organizing Systems*, pp. 141–148, IEEE, 2013.
- [39] Y. Khaluf, S. Van Havermaet, and P. Simoens, "Collective lévy walk for efficient exploration in unknown environments," in *Artificial Intelligence: Methodology, Systems, and Applications: 18th International Conference, AIMSA 2018, Varna, Bulgaria, September 12–14, 2018, Proceedings 18*, pp. 260–264, Springer, 2018.
- [40] C. Pinciroli, V. Trianni, R. O'Grady, G. Pini, A. Brutschy, M. Brambilla, N. Mathews, E. Ferrante, G. Di Caro, F. Ducatelle, et al., "Argos: a modular, parallel, multi-engine simulator for multi-robot systems," *Swarm intelligence*, vol. 6, pp. 271–295, 2012.
- [41] M. Allwright, N. Bhalla, C. Pinciroli, and M. Dorigo, "Argos plugins for experiments in autonomous construction," tech. rep., Tech. Rep. TR/IRIDIA/2018-007, IRIDIA, Université Libre de Bruxelles . . . , 2018.
- [42] M. Allwright, N. Bhalla, C. Pinciroli, and M. Dorigo, "Simulating multi-robot construction in argos," in *International Conference on Swarm Intelligence*, pp. 188–200, Springer, 2018.